

## Cu<sup>2+</sup> Coordination Properties of a 2-Pyridine Heptaamine Tripod: Characterization and Binding Mechanism

Alejandra Sornosa Ten,<sup>†</sup> Nicolas Humbert,<sup>†</sup> Begoña Verdejo,<sup>‡</sup> José M. Linares,<sup>§</sup> Mourad Elhabiri,<sup>†</sup> Julia Jezierska,<sup>||</sup> Conxa Soriano,<sup>‡</sup> Henryk Kozlowski,<sup>||</sup> Anne-Marie Albrecht-Gary,<sup>\*†</sup> and Enrique García-España<sup>\*‡</sup>

<sup>†</sup>Laboratoire de Physico-Chimie Bioinorganique, Institut de Chimie, UMR 7177 CNRS-UdS, Université de Strasbourg, ECPM 25, rue Becquerel, 67200 Strasbourg, France, <sup>‡</sup>Instituto de Ciencia Molecular (ICMOL), Departamentos de Química Inorgánica y Orgánica, Universidad de Valencia, Edificio de Institutos, Apartado de Correos 22085, 46071 Valencia, Spain, <sup>§</sup>Instituto de Ciencia Molecular (ICMOL), Departamento de Química Orgánica, Fundació General de la Universidad de Valencia, Spain, and <sup>||</sup>Faculty of Chemistry, University of Wrocław, 14 Joliot-Curie St, 50-383 Wrocław, Poland

Received June 6, 2009

The synthesis, protonation, and Cu<sup>2+</sup> coordination chemistry of a tripodal heptaamine ligand (**L**<sup>1</sup>) functionalized with 2-pyridine fragments at the ends of its three branches are reported. **L**<sup>1</sup> presents six relatively high protonation constants followed by much more reduced constant that as indicated by the UV–vis and NMR data, occur on the pyridine fragments. p[H]-metric, ESI/MS<sup>+</sup>, EPR and UV–vis data show that **L**<sup>1</sup> is able to form mono-, di-, and trinuclear Cu<sup>2+</sup> complexes. Slippage movements and molecular reorganizations have been observed to occur as a function of p[H] in the 1:1 Cu<sup>2+</sup> complexes. The kinetic studies showed that the complex formation is fast and proceeds through a dissociative Eigen–Wilkins mechanism. The decomposition of Cu**L**<sup>1</sup> upon addition of acid excess occurs with two separate kinetic steps; the rate constant for the fast process does not vary with respect to the H<sup>+</sup> concentration whereas a linear dependence on H<sup>+</sup> is observed for the slow step.

### Introduction

The polyamine *N,N*-bis(2-aminoethyl)ethane-1,2-diamine usually named with the non-systematic name tris(2-aminoethyl)amine and abbreviated as *tren*, constitutes one of the ligands most widely employed within the fields of Coordination and Supramolecular Chemistry.<sup>1</sup> This interest stems from its tripodal disposition which frequently favors rhombic geometries and from the facility of its derivatization that permits one to obtain related ligands for a variety of purposes. For instance, *tren* derivatives containing additional carboxylate, catecholate, or hydroxamate groups have been used as synthetic sidero-

phores for binding Fe<sup>3+</sup>,<sup>2–4</sup> or as Gd<sup>3+</sup> chelators for preparing contrast agents for magnetic resonance imaging (MRI).<sup>5–7</sup> *Tren* or *tren*-like fragments have also been used as building blocks of more or less sophisticated supramolecular receptors of either acyclic or cyclic topology endowed with interesting coordinative or/and photochemical properties.<sup>8–10</sup>

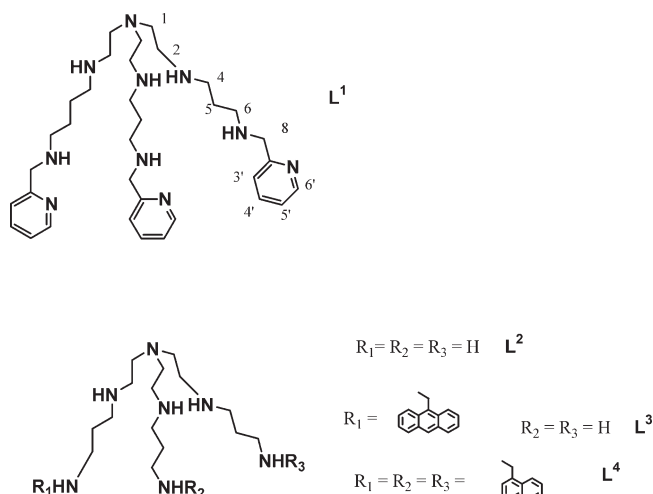
Within this context, some of us have prepared several new polyamine ligands built up by expanding the *tren* structure with aminopropyl chains (**L**<sup>2</sup>), and further functionalizing the terminal primary nitrogens with one methylanthryl

\*To whom correspondence should be addressed. E-mail: enrique.garcia-es@uv.es.

- (1) Blackman, A. G. *Polyhedron* 2005, 24, 1–39.
- (2) (a) Blanc, S.; Yakirevitch, P.; Leize, E.; Meyer, M.; Libman, J.; Van Dorsselaer, A.; Albrecht-Gary, A.-M.; Shanzer, A. *J. Am. Chem. Soc.* 1997, 119, 4934–4944. (b) Albrecht-Gary, A.-M.; Blanc, S.; Biaso, F.; Thomas, F.; Baret, P.; Gelon, G.; Pierre, J.-L.; Serratrice, G. *Eur. J. Inorg. Chem.* 2003, 2596–2605.
- (3) (a) Karpishin, T. B.; Stack, T. D. P.; Raymond, K. N. *J. Am. Chem. Soc.* 1993, 115, 6115–6125. (b) Xu, J.; O'Sullivan, B.; Raymond, K. N. *Inorg. Chem.* 2002, 41, 6731–6742. (c) Hajela, S. P.; Johnson, A. R.; Xu, J.; Sunderland, C. J.; Coehn, S. M.; Caulder, D. L.; Raymond, K. N. *Inorg. Chem.* 2001, 40, 3208–3216.
- (4) Tor, Y.; Libman, J.; Shanzer, A.; Lifson, S. *J. Am. Chem. Soc.* 1987, 109, 6517–6518.

- (5) (a) Doble, D. M. J.; Botta, M.; Wang, J.; Aime, S.; Barge, A.; Raymond, K. N. *J. Am. Chem. Soc.* 2001, 123, 10758–10759. (b) Cohen, S. M.; Xu, J.; Radkov, E.; Raymond, K. N.; Botta, M.; Brage, A.; Aime, S. *Inorg. Chem.* 2000, 39, 5747–5756.
- (6) Bretonniere, Y.; Mazzanti, M.; Pécaut, J.; Dunand, F. A.; Merbach, A. E. *Inorg. Chem.* 2001, 40, 6737–6745.
- (7) Blake, A. J.; Doble, D. J. M.; Li, W.-A.; Schröder, M. *J. Chem. Soc., Dalton Trans.* 1987, 3655–3658.
- (8) (a) Sohna Sohna, J.-E.; Carrier, V.; Fages, F.; Amouyal, E. *Inorg. Chem.* 2001, 40, 6061–6063. (b) Prodi, L.; Bolletta, F.; Montalti, M.; Zaccheroni, N. *Eur. J. Inorg. Chem.* 1999, 455–460.
- (9) (a) Comba, P.; Lampeka, Y. D.; Nazarenko, A. Y.; Prikhodko, A. I.; Pritkow, H.; Taraszewska, J. *Eur. J. Inorg. Chem.* 2002, 1871–1882. (b) Bencini, A.; Berni, E.; Bianchi, A.; Giorgi, C.; Valtancoli, B.; Chand, D. K.; Schneider, H.-J. *J. Chem. Soc., Dalton Trans.* 2003, 793–800. (c) Amendola, V.; Fabbrizzi, L.; Mangano, C.; Lanfredi, A. M.; Pallavicini, P.; Perotti, A.; Ugozzoli, F. *J. Chem. Soc., Dalton Trans.* 2000, 1155–1160.

Chart 1



fragment ( $L^3$ ) or with three methylnaphthyl fragments ( $L^4$ ) (Chart 1).<sup>11</sup> These compounds exhibited interesting properties in their coordination chemistry with  $Cu^{2+}$  and in their anion coordination capabilities toward nucleotidic anions. Furthermore, compound  $L^4$  showed an appealing photochemical behavior with the formation of an excimer species of very strong intensity.<sup>12</sup>

Following along with this research, we have now prepared a new  $L^1$  polyamine receptor made up by attaching three 2-methylpyridine units to the primary nitrogens of the enlarged polyamine  $L^2$  (Chart 1) so that different binding sites can be present within the tripod structure with the possibility of forming coordinatively unsaturated trinuclear complexes. Here in this first report on the chemistry of this new polyamine, we describe its synthesis, protonation behavior, and  $Cu^{2+}$  coordination chemistry using potentiometric, ESI/MS<sup>+</sup>, UV-vis, EPR, and kinetic techniques.

## Experimental Section

**Synthesis of Tris(8-(2'-pyridyl)-3,7-diazaoctyl)amine ( $L^1 \cdot 7HCl$ ).** Tris(3,7-diazaoctyl)amine ( $L^2$ ) (2.8 g, 8.82 mmol) and pyridine-2-carbaldehyde (3.18 g, 29.69 mmol) were stirred for 1.5 h in 200 mL of dry EtOH.  $NaBH_4$  (3.21 g, 84.47 mmol) was then added, and the resulting solution was stirred for 2 h at room temperature. The solvent was removed at reduced pressure. The resulting residue was treated with water and dichloromethane. The organic phase was removed at reduced pressure, and the resulting residue was dissolved in dry ethanol and precipitated as its hydrochloride salt of tris(8-(2'-pyridyl)-3,7-diazaoctyl)amine

( $L^1$ ) (yield 54%).  $^1H$  NMR ( $D_2O$ ),  $\delta$ (ppm): 2.12–2.20 (m, 2H), 2.86 (t,  $J = 6$  Hz, 2H), 3.08–3.24 (m, 6H), 4.44 (s, 2H), 7.54 (d, d,  $J_1 = 8$  Hz,  $J_2 = 8$  Hz,  $J_3 = 2$  Hz, 1H), 7.59 (d,  $J_1 = 8$  Hz, 1H), 8.01 (d, d, d,  $J_1 = J_2 = 8$  Hz,  $J_3 = 2$  Hz, 1H), 8.58 (d,  $J_1 = 8$  Hz, 1H).  $^{13}C$  NMR ( $D_2O$ ),  $\delta$ (ppm): 22.9, 44.6, 44.9, 45.2, 49.1, 51.3, 124.6, 125.1, 149.5. Anal. Calcd for  $C_{33}H_{54}N_{10} \cdot 7HCl$ : C, 45.27%, H, 7.13%, N, 15.99%. Found: C, 45.2%, H, 7.2%, N, 16.2%.

**emf Measurements.** The potentiometric titrations were carried out at 298.1(1) K in 0.15 mol  $dm^{-3}$  ( $NaClO_4$ ). The experimental procedure used (buret, potentiometer, cell, stirrer, microcomputer, etc.) was the same that has been fully described elsewhere.<sup>13</sup> The acquisition of the emf data was performed with the computer program PASAT.<sup>14</sup> The reference electrode was an Ag/AgCl electrode in saturated KCl solution. The glass electrode was calibrated as an hydrogen-ion concentration probe by titration of previously standardized amounts of HCl with  $CO_2$ -free NaOH solutions and determining the equivalent point by the Gran's method,<sup>15</sup> which gives the standard potential,  $E^\circ$ , and the ionic product of water ( $pK_w = 13.73(1)$ ). The concentrations of the stock  $Cu^{2+}$  solutions employed were determined gravimetrically by standard methods.<sup>16</sup> The p[H] range investigated was 2.5–11.0, and the concentration of  $Cu^{2+}$  and ligands ranged from  $1 \times 10^{-3}$  to  $5 \times 10^{-3}$  mol  $dm^{-3}$  with M/L molar ratios varying from 1:1 to 3:1. Precipitation was observed above pH 7 for  $Cu^{2+}/L$  3:1 solutions.

The computer program HYPERQUAD<sup>17</sup> was used to calculate the protonation and stability constants. The different titration curves for each system (at least two titrations) were treated either as a single set or as separated curves without significant variations in the values of the stability constants. The sets of data were merged together and treated simultaneously to give the final stability constants. All the distribution diagrams have been calculated with the computer program HYSS.<sup>18</sup>

**Electrospray Mass Spectrometry.** Electrospray mass spectra were recorded on a Bruker Esquire 3000plus, Bruker Daltonics mass spectrometer (Agilent Headquarters, Palo Alto, U.S.A.). ESI/MS<sup>+</sup> was carried out in the positive ion mode. Scanning was performed from  $m/z = 100$  to 1500. For electrospray ionization, the drying gas was set at a flow rate of 2.5  $\mu L/min$ , with capillary voltage of 280 V. Non-buffered solutions containing  $Cu^{2+}:L^1$  ( $[L^1] = 9.75 \times 10^{-5}$  mol  $dm^{-3}$ , molar ratios 1:1, 2:1, and 3:1) in water were injected into the mass spectrometer source with a syringe pump (Cole-Parmer Instruments Company, Illinois, U.S.A.) at a flow rate of 5 L/min. The sampling skimmer voltage ( $V_s$ ) was set at 40 V.

**UV-vis Titrations.** All solutions were prepared with deionized water, and the ionic strength was fixed at 0.15 mol  $dm^{-3}$  using  $NaClO_4$  (Merck, p.a.).  $L^1$  or its copper complexes were dissolved and introduced into a jacketed cell (20 mL) maintained at 298.1(1) K using a Haake FJ thermostat. The solutions were deoxygenated and flushed continuously with argon during the titrations. The free hydrogen concentrations were measured with an Ag/AgCl combined glass electrode (Metrohm 6.0234.500, long life and a Tacussel Isis 20 000 millivoltmeter). Standardization of the millivoltmeter and verification of the linearity of the electrode were performed using commercial

(10) (a) Lamarque, L.; Navarro, P.; Miranda, C.; Aran, V. J.; Ochoa, C.; Escarti, F.; García-España, E.; Latorre, J.; Luis, S. V.; Miravet, J. F. *J. Am. Chem. Soc.* **2001**, *123*, 10560–10570. (b) Clares, M. P.; Aguilar, J.; Aucejo, R.; Lodeiro, C.; Albelda, M. T.; Pina, F.; Lima, J. C.; Parola, A. J.; Pina, J.; Seixas, J.; Soriano, C.; García-España, E. *Inorg. Chem.* **2004**, *43*, 6114–6122. (c) Balzani, V.; Campagna, S.; Denti, G.; Juris, A.; Serroni, S.; Venturi, M. *Acc. Chem. Res.* **1998**, *31*, 26–34. (d) Vogtle, F.; Gestermann, S.; Kauffmann, C.; Ceroni, P.; Vicinelli, V.; Balzani, V. *J. Am. Chem. Soc.* **2000**, *122*, 10398–10404.

(11) (a) Seixas, J.; Pina, J.; Pina, F.; Lodeiro, C.; Parola, A. J.; Lima, J. C.; Albelda, M. T.; Clares, M. P.; García-España, E.; Soriano, C. *J. Phys. Chem. A* **2003**, *107*, 11307–11318. (b) Lomadze, N.; Schneider, H.-J.; Albelda, M. T.; García-España, E.; Verdejo, B. *Org. Biomol. Chem.* **2006**, 1755–1759. (c) Albelda, M. T.; García-España, E.; Jiménez, H. R.; Llinares, J.-M.; Soriano, C.; Sornosa Ten, A.; Verdejo, B. *J. Chem. Soc., Dalton Trans.* **2006**, 4474–4481.

(12) Albelda, M. T.; García-España, E.; Gil, L.; Lima, J. C.; Lodeiro, C.; Seixas de Melo, J.; Melo, M. J.; Parola, A. J.; Pina, F.; Soriano, C. *J. Chem. Phys. B* **2003**, *107*, 6573–6578.

(13) García-España, E.; Ballester, M.-J.; Lloret, F.; Moratal, J. M.; Faus, J.; Bianchi, A. *J. Chem. Soc., Dalton Trans.* **1988**, 101–104.

(14) Fontanelli M.; Micheloni, M. Proceedings of the Spanish-Italian Congress on Thermodynamic of Metal Complexes, Diputación de Castellón, Castellón, Spain, 1990.

(15) (a) Gran, G. *Analyst* **1952**, *77*, 661–671. (b) Rossotti, F. J. C.; Rossotti, H. *J. Chem. Educ.* **1965**, *42*, 375–378.

(16) Gridley, D. N. *An Advanced Course in Practical Inorganic Chemistry*; Butterworths: London, 1964.

(17) Gans, P.; Sabatini, A.; Vacca, A. *Talanta* **1996**, *43*, 1739–1753.

(18) HYPERQUAD Simulation and Speciation (HySS) Protonic Software; P. Gans, Protonic Software: 2 Templegate Avenue, Leeds LS15 0HD, England, 2006.

Merck buffered solutions ( $p[H] = 1.68, 4.00, 6.86, 7.41, \text{ and } 9.18$ ) according to classical methods.

The titrations of the free ligand ( $5.48 \times 10^{-5} \text{ mol dm}^{-3}$ ) and of its  $\text{Cu}^{2+}$  complexes (concentrations of  $\text{L}^1$  were  $6.22 \times 10^{-5} \text{ mol dm}^{-3}$ ,  $4.74 \times 10^{-5} \text{ mol dm}^{-3}$ , and  $3.38 \times 10^{-5} \text{ mol dm}^{-3}$  for metal/ligands molar ratios 1:1, 2:1, and 3:1, respectively) with  $pH$  were carried out by addition of known volumes of sodium hydroxide ( $0.1 \text{ mol dm}^{-3}$ , Merck, Titrisol) with a piston-fitted microburet (Manostat). Simultaneous  $p[H]$  and UV-vis measurements were performed. For this set of titrations, the absorption spectra ( $l = 1 \text{ cm}$ ) were recorded in the 200–400 nm wavelength range using a CARY 50 (Varian) equipped with Hellma optical fibers (Hellma, 041.002-UV) and an immersion probe made of quartz suprazil (Hellma, 661.500-QX).

A second set of titrations was carried out for the copper complexes in the 500–800 nm spectral range. The concentrations of  $\text{L}^1$  were  $9.20 \times 10^{-4} \text{ mol dm}^{-3}$  ( $l = 1 \text{ cm}$ ),  $1.19 \times 10^{-3} \text{ mol dm}^{-3}$  ( $l = 2 \text{ cm}$ ), and  $8.05 \times 10^{-4} \text{ mol dm}^{-3}$  ( $l = 1 \text{ cm}$ ) for molar ratios metal/ligands 1:1, 2:1, and 3:1, respectively. The spectra were recorded with a Uvikon 941 (Kontron) spectrophotometer from 500 and 800 nm using quartz optical cell (Hellma).

To determine the apparent stability constants and to establish the most appropriate conditions for the kinetic measurements (see below and in the Results and Discussion section), a couple of titration sets were performed at fixed  $pH$  values adding increasing amounts of metal ion to fixed concentrations of  $\text{L}^1$ . In the first set, the  $p[H]$  of the solution was fixed at 5.45 by MES (2-(*N*-morpholine)ethanesulfonic acid,  $0.1 \text{ mol dm}^{-3}$ ). Aliquots of a solution of  $\text{Cu}^{2+}$  ( $5.03 \times 10^{-3} \text{ mol dm}^{-3}$ ) were added to a quartz cell of 1 cm path length containing 2 mL of a buffered solution of  $\text{L}^1$  ( $4.62 \times 10^{-5} \text{ mol dm}^{-3}$ ) until the ratio  $[\text{Cu}^{2+}]_{\text{tot}}/[\text{L}^1]_{\text{tot}} = 3.90$  was attained. A spectrum was recorded in the 220–400 nm range after each addition of  $\text{Cu}^{2+}$ . In the second set, the  $p[H]$  was fixed at 2.39 using a  $4 \times 10^{-3} \text{ mol dm}^{-3}$   $\text{HClO}_4$  solution. Different volumes of a  $5.06 \times 10^{-2} \text{ mol dm}^{-3}$  copper solution were added to 4 mL of a  $4.20 \times 10^{-4} \text{ mol dm}^{-3}$  solution of  $\text{L}^1$  until the ratio  $[\text{Cu}^{2+}]_{\text{tot}}/[\text{L}^1]_{\text{tot}} = 5.43$  was obtained. A spectrum ( $l = 2 \text{ cm}$ ) was registered in the 500–800 nm range after each addition. For both sets of titrations a Uvikon 941 (Kontron) spectrophotometer was used.

All the spectrophotometric data were processed with the SPECFIT program,<sup>19</sup> which adjusts the stability constants and the corresponding molar extinction coefficients ( $\text{mol}^{-1} \text{ dm}^3 \text{ cm}^{-1}$ ) of the species at equilibrium. SPECFIT uses factor analysis to reduce the absorbance matrix and to extract the eigenvalues prior to the multiwavelength fit of the reduced data set according to the Marquardt algorithm.

**EPR Measurements.** Electron paramagnetic resonance (EPR) spectra were performed in ethylene glycol–water (30/70, v/v) solution at 77 K on a Bruker ESP 300E spectrometer at the X-band frequency (9.45 GHz) and equipped with the Bruker NMR gaussmeter ER 035 M and the Hewlett-Packard microwave frequency counter HP 5350B. The metal concentration was adjusted to  $3 \times 10^{-3} \text{ mol dm}^{-3}$ , and the metal-to-ligand concentration ratios were 1:1, 2:1, and 3:1. The experimental EPR spectra were analyzed using computer simulation programs.<sup>20</sup>

(19) (a) SPECFIT, A Program for Global Least Square Fitting of Equilibrium and Kinetic Systems using Factor Analysis and Marquardt Minimization, Version 1–26; 4 Spectrum Software Associates: Chapel Hill, NC, 1996. (b) Gampp, H.; Maeder, M.; Meyer, C. J.; Zuberhuhler, A. D. *Talanta* **1985**, *32*, 95–101. (c) Gampp, H.; Maeder, M.; Meyer, C. J.; Zuberhuhler, A. D. *Talanta* **1985**, *32*, 257–264. (d) Gampp, H.; Maeder, M.; Meyer, C. J.; Zuberhuhler, A. D. *Talanta* **1986**, *33*, 943–951.

(20) (a) Ozarowski, A. National High Magnetic Field Laboratory, Florida State University, Tallahassee, FL, unpublished program. (b) SimFonia, version 1.25; Bruker AXS: Madison, WI.

**Table 1.** Logarithms of the Stepwise Protonation Constants for the Ligand  $\text{L}^1$  Determined at 298.1(1) K in  $0.15 \text{ mol dm}^{-3} \text{ NaClO}_4$ <sup>a</sup>

entry	reaction <sup>b</sup>	$\text{L}^1$	$\text{L}^2$
		$\log K (\sigma)$	$\log K (\sigma)^c$
1	$\text{L} + \text{H} \rightleftharpoons \text{HL}$	10.06(2)	10.34(7) <sup>c</sup>
2	$\text{HL} + \text{H} \rightleftharpoons \text{H}_2\text{L}$	9.41(1)	10.26(2)
3	$\text{H}_2\text{L} + \text{H} \rightleftharpoons \text{H}_3\text{L}$	8.53(1)	9.52(4)
4	$\text{H}_3\text{L} + \text{H} \rightleftharpoons \text{H}_4\text{L}$	7.52(1)	8.68(4)
5	$\text{H}_4\text{L} + \text{H} \rightleftharpoons \text{H}_5\text{L}$	7.05(1)	7.91(5)
6	$\text{H}_5\text{L} + \text{H} \rightleftharpoons \text{H}_6\text{L}$	6.33(1)	7.34(4)

<sup>a</sup> The corresponding protonation constants for  $\text{L}^2$  are included for comparison. <sup>b</sup> Charges are omitted for the sake of clarity. <sup>c</sup> Taken from ref 11c.

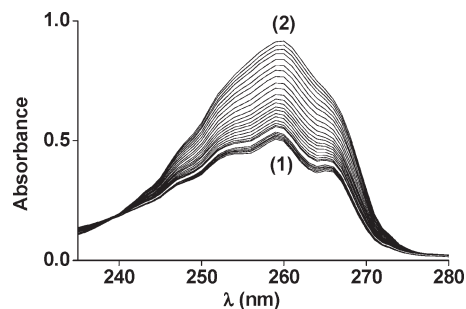


**Figure 1.** Spectrophotometric titration of  $\text{L}^1$  vs  $p[H]$  recorded in  $\text{H}_2\text{O}$ ;  $T = 298.1(1) \text{ K}$ ;  $l = 1 \text{ cm}$ ;  $l = 1.0 \text{ mol dm}^{-3} (\text{NaClO}_4)$ ;  $[\text{L}^1]_{\text{tot}} = 5.48 \times 10^{-5} \text{ mol dm}^{-3}$ ; (1)  $p[H] = 3.41$ ; (2)  $p[H] = 1.15$ .

**Kinetic Experiments.** A stopped-flow spectrophotometer (Applied Photophysics SX-18MV) was used for the fast kinetics experiments. The temperature was maintained at 298.1(1) K with a Haake thermostat. Formation kinetics were studied at two different  $p[H]$  values, 2.39 and 5.45. The wavelengths used at  $p[H] = 2.39$  and  $p[H] = 5.45$  were 600 and 285 nm, respectively, with an optical path length of 1 cm.

The solutions of free ligand and  $\text{Cu}^{2+}$  were prepared in water where the  $p[H]$  was fixed at  $p[H] = 2.39$  with  $4 \times 10^{-3} \text{ mol dm}^{-3} \text{ HClO}_4$ . The ligand concentration was fixed at  $2.10 \times 10^{-4} \text{ mol dm}^{-3}$ , and the copper concentrations were varied from  $2.10 \times 10^{-3}$  to  $2.25 \times 10^{-2} \text{ mol dm}^{-3}$ . For  $p[H] = 5.45$  (MES buffer,  $0.1 \text{ mol dm}^{-3}$ ), the total concentration of ligand was  $2.31 \times 10^{-5} \text{ mol dm}^{-3}$ , and the copper concentrations were varied from  $4.15 \times 10^{-4} \text{ mol dm}^{-3}$  to  $1.31 \times 10^{-3} \text{ mol dm}^{-3}$ . At least 10 times more concentrated solutions of  $\text{Cu}^{2+}$  were used to obtain pseudo-first order conditions. Three reproducible experiments were carried out with different  $\text{Cu}^{2+}$  concentrations, and all the data were correctly fitted with a mono-exponential equation.

The dissociation reaction of the copper complex ( $[\text{CuL}^1] = 4.39 \times 10^{-5} \text{ mol dm}^{-3}$ ) maintained at 298.1(1) K (Lauda M12 thermostat) was monitored on a SX-18MV stopped-flow spectrophotometer (Applied Photophysics). Pseudo-first order conditions with respect to the complex were used, and acid ( $\text{HClO}_4$ ) concentration was varied from  $1.11 \times 10^{-3} \text{ mol dm}^{-3}$  to  $9.2 \times 10^{-3} \text{ mol dm}^{-3}$ . The absorbance decay versus time was monitored at 285 nm with a 1 cm optical cell.

All kinetic data sets, averaged out of at least three replicates, were analyzed with the commercial software BIOCINE.<sup>21</sup> This program fits up to three exponential functions to the experimental curves with the Simplex algorithm after initialization with a Padé-Laplace method.

(21) (a) Biokine V 3.0, User's Manual; Bio-Logic: Echirrolles, 1991. (b) Nelder, J. A.; Mead, R. *Computer J.* **1965**, *7*, 308–313. (c) Yeramian, E.; Claverie, P. *Nature* **1987**, *326*, 169–174.

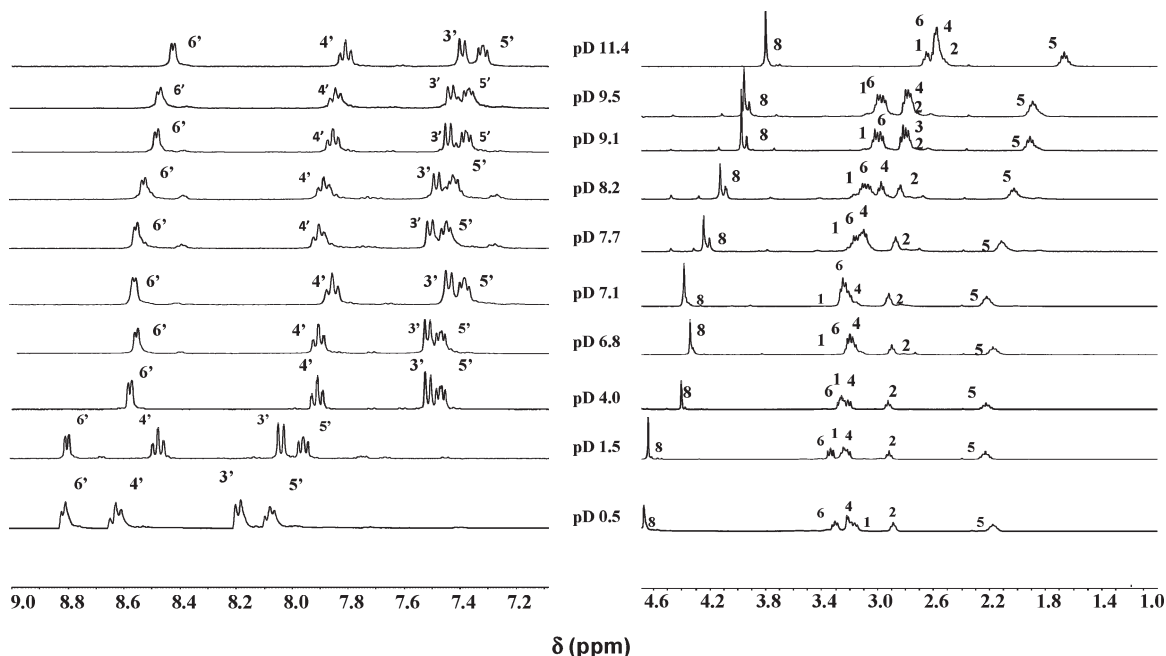
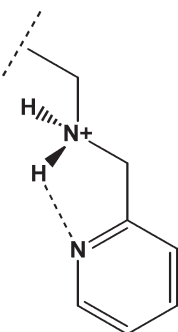


**Figure 2.** Variation of the chemical shifts of the  $^1\text{H}$  signals of  $\text{L}^1$  with the pD.

#### Chart 2



### Results and Discussion

**Ligand Protonation Equilibria.** The behavior of  $\text{L}^1$  toward protonation has been studied by potentiometry in  $0.15 \text{ mol dm}^{-3} \text{ NaClO}_4$  at  $298.1(1) \text{ K}$  in the  $2.5\text{--}11.0$  p[H] range. The values of the stepwise basicity constants obtained for  $\text{L}^1$  are presented in Table 1 along with those previously reported for its synthetic precursor  $\text{L}^2$ .<sup>11</sup> The distribution diagram for the system  $\text{L}^1\text{--H}^+$  is shown in the Supporting Information, Figure S1.

In the p[H] range in which the potentiometric studies were carried out  $\text{L}^1$  takes up six protons. The hexaprotonated species  $[\text{H}_6\text{L}^1]^{6+}$  prevails over a wide p[H] range  $2.0\text{--}6.0$  (Supporting Information, Figure S1).

$\text{L}^1$  shows a reduced basicity in all its protonation steps with respect to  $\text{L}^2$ , which can be largely attributed to the electron withdrawing character of the pyridine rings and to the fact that  $\text{L}^2$  contains primary amino terminal groups. It is well-known that primary amino groups have more favorable hydration energy and thereby better

stabilize the positive charges.<sup>22,23</sup> Similar effects have been reported for other open-chain polyamines functionalized at their ends with 2-picolyl groups.<sup>24,25</sup>

To check whether the pyridine nitrogens bear a neat protonation or not at acidic p[H] values, we have carried out a spectrophotometric study of this system.  $\text{L}^1$  presents a structured absorption band centered at about  $257 \text{ nm}$  that can be ascribed to a  $\pi\text{--}\pi^*$  transitions of the pyridine ring.<sup>26</sup> The sharp increase observed in the absorbance when the p[H] is decreased below 3 (Figure 1) confirms the protonation of the pyridine rings at these p[H] values. The statistical analysis<sup>19</sup> of the UV data led to the determination of a global constant with a value of  $\log \beta = 5.77(7)$  that implies three protons corresponding to the protonation of the three pyridine nitrogens ( $[\text{H}_6\text{L}^1]^{6+} + 3\text{H}^+ \rightleftharpoons [\text{H}_9\text{L}^1]^{9+}$ ). The calculated spectra of free  $\text{L}^1$  and of its protonated forms ( $[\text{H}_6\text{L}^1]^{6+}$  and  $[\text{H}_9\text{L}^1]^{9+}$ ) are shown in Supporting Information, Figure S2. The averaged protonation constant ( $\log K = 5.77/3 - 1.92$ ) for the pyridine units of  $\text{L}^1$  is very low in comparison with that measured for the free pyridine ring ( $\log K = 5.24$ ).<sup>25</sup>

It is well established that, upon protonation of polyamine compounds, the carbon atom in  $\beta$ -position and the hydrogen nuclei attached to the carbon atom in  $\alpha$ -position to the nitrogen atom undergoing protonation are those exhibiting, respectively, the largest upfield and

(22) (a) Lu, Q.; Caroll, R. I.; Reibenspies, J. H.; Martell, A. E.; Clearfield, A. *J. Mol. Struct.* **1988**, *470*, 121–134. (b) Szwajca, A.; Leska, B.; Schroeder, G.; Szafran, M. *J. Mol. Struct.* **2004**, *708*, 87–95. (c) Koné, M.; Illien, B.; Laurence, C.; Gal, J.-F.; Maria, P.-C. *J. Phys. Org. Chem.* **2006**, *19*, 104–114. (d) Schafman, B. S.; Wenthold, P. G. *J. Org. Chem.* **2007**, *72*, 1645–1651.

(23) Bencini, A.; Bianchi, A.; García-España, E.; Micheloni, M.; Ramírez, J. A. *Coord. Chem. Rev.* **1999**, *188*, 97–156. (b) Frassinetti, C.; Alderighi, L.; Gans, P.; Sabatini, A.; Vacca, A.; Ghelli, S. *Anal. Bioanal. Chem.* **2003**, *376*, 1041–1052. (c) Samesky, J. E.; Surprenant, H. L.; Molen, F. K.; Reilley, C. N. *Anal. Chem.* **1975**, *47*, 2116–2124. (d) Hague, D. N.; Moreton, A. D. *J. Chem. Soc., Perkin Trans. 2.* **1994**, 265–270.

(24) Harris, W. R.; Murase, I.; Timmons, J. H.; Martell, A. E. *Inorg. Chem.* **1978**, *17*, 889–894.

(25) Smith, R. M.; Martell, A. E. *NIST Stability Constants Database*, version 4.0; National Institute of Standards and Technology: Washington, DC, 1997.

(26) Mohamadou, A.; Gerard, C. *J. Chem. Soc., Dalton Trans.* **2001**, 3320–3328.

**Table 2.** Stability Constants for the  $\text{Cu}^{2+}$  Complexes Formed with  $\text{L}^1$  Determined in  $0.15 \text{ mol dm}^{-3} \text{ NaClO}_4$  at  $298.1(1) \text{ K}^a$ 

entry	reaction <sup>b</sup>	$\text{L}^1$	$\text{L}^2$
		$\log K (\sigma)$	$\log K (\sigma)^{11c}$
1	$\text{Cu} + \text{L} \rightleftharpoons \text{CuL}$	21.2(2)	22.91(4)
2	$\text{CuL} + \text{H} \rightleftharpoons \text{CuHL}$	8.20(2)	9.52(3)
3	$\text{CuHL} + \text{H} \rightleftharpoons \text{CuH}_2\text{L}$	7.42(1)	9.21(2)
4	$\text{CuH}_2\text{L} + \text{H} \rightleftharpoons \text{CuH}_3\text{L}$	5.52(2)	3.96(2)
5	$\text{CuH}_3\text{L} + \text{H} \rightleftharpoons \text{CuH}_4\text{L}$	4.24(1)	
6	$\text{CuL} + \text{Cu} \rightleftharpoons \text{Cu}_2\text{L}$	10.56(3)	7.84(6)
7	$\text{Cu}_2\text{L} + \text{H} \rightleftharpoons \text{Cu}_2\text{HL}$	6.45(2)	
8	$\text{Cu}_2\text{L} + 2\text{H}_2\text{O} \rightleftharpoons \text{Cu}_2\text{L}(\text{OH})_2 + 2\text{H}$	$\log \beta = -20.42(3)$	$\log \beta = -19.99(6)$
9	$\text{Cu}_2\text{L} + \text{Cu} \rightleftharpoons \text{Cu}_3\text{L}$	6.56(3)	
10	$\text{Cu}_3\text{L} + \text{H} \rightleftharpoons \text{Cu}_3\text{HL}$	3.64(3)	

<sup>a</sup> Selected equilibrium constants for the system  $\text{Cu}^{2+} - \text{L}^2$  are included for comparison. <sup>11c</sup> <sup>b</sup> Charges are omitted for the sake of clarity.

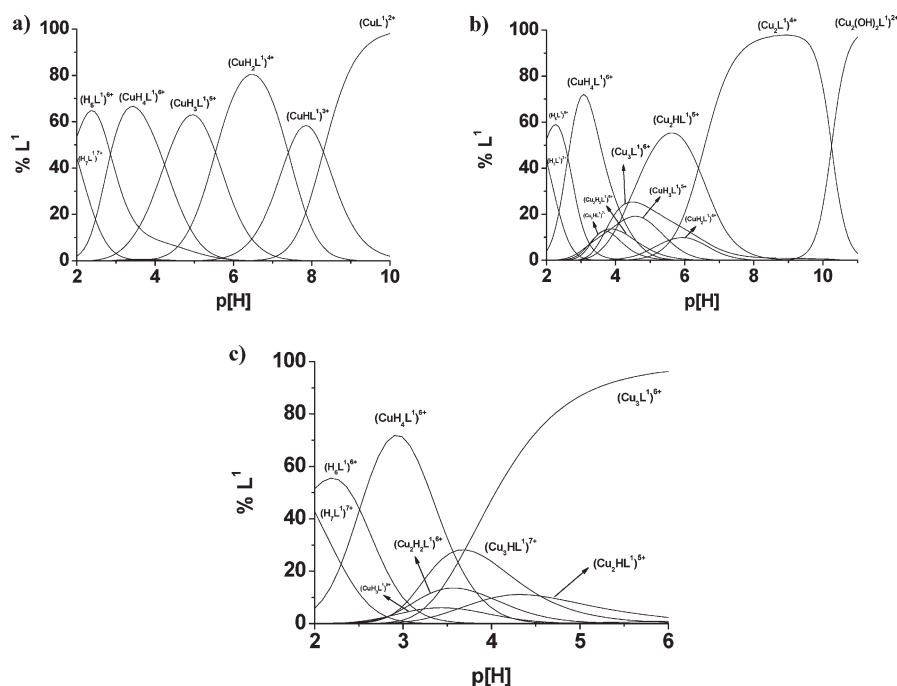


**Figure 3.** Ligand distribution diagrams for the system  $\text{Cu}^{2+}/\text{L}^1$  as a function of pH. (a)  $[\text{Cu}^{2+}]_{\text{tot}} = [\text{L}^1]_{\text{tot}} = 1 \times 10^{-3} \text{ mol dm}^{-3}$ ; (b)  $[\text{Cu}^{2+}]_{\text{tot}} = 2 \times 10^{-3} \text{ mol dm}^{-3}$ ;  $[\text{L}^1]_{\text{tot}} = 1 \times 10^{-3} \text{ mol dm}^{-3}$ ; (c)  $[\text{Cu}^{2+}]_{\text{tot}} = 3 \times 10^{-3} \text{ mol dm}^{-3}$ ;  $[\text{L}^1]_{\text{tot}} = 1 \times 10^{-3} \text{ mol dm}^{-3}$ . The averaged protonation constant ( $\log K = 5.77/3 - 1.92$ ) for the pyridine units of  $\text{L}^1$  has been used as an estimate of  $\log K_{\text{L}^1\text{H}_3}$ .

**Table 3.** Attribution of the Peaks Observed in the ESI/MS<sup>+</sup> Experiments

ions	calculated, $m/z$	experimental, $m/z$	$[\text{Cu}(\text{II})]_{\text{tot}}/[\text{L}^1]_{\text{tot}}$		
			1.0	2.0	3.0
$[\text{L} + \text{Cu} + \text{Cl}]^+$	688.4	688.3	×		
$[\text{L} + \text{Cu} + \text{ClO}_4]^+$	752.3	752.1	×	×	×
$[\text{L} + \text{Cu} + \text{Cl} + \text{ClO}_4 + \text{H}]^+$	788.3	788.2	×		
$[\text{L} + 2\text{Cu} + \text{ClO}_4 - 2\text{H}]^+$	813.3	813.1	×		
$[\text{L} + 2\text{Cu} + \text{Cl} + \text{ClO}_4]^+{}^a$	850.3	850.2		×	×
$[\text{L} + \text{Cu} + 2\text{ClO}_4 + \text{H}]^+$	852.3	852.1	×		
$[\text{L} + 2\text{Cu} + 2\text{Cl} + \text{ClO}_4]^+$	885.1	885.0	×	×	×
$[\text{L} + 2\text{Cu} + \text{Cl} + 2\text{ClO}_4]^+$	949.2	949.0	×	×	×
$[\text{L} + 3\text{Cu} + 3\text{Cl} + \text{ClO}_4 + 2\text{H}]^+{}^a$	985.1	984.9		×	×
$[\text{L} + 2\text{Cu} + 3\text{ClO}_4]^+$	1013.0	1013.2		×	×
$[\text{L} + 3\text{Cu} + 2\text{Cl} + 2\text{ClO}_4 + 2\text{H}]^+{}^a$	1049.1	1048.9		×	×
$[\text{L} + 3\text{Cu} + 3\text{Cl} + 2\text{ClO}_4]^+$	1082.1	1082.0		×	×
$[\text{L} + 3\text{Cu} + \text{Cl} + 3\text{ClO}_4 + 2\text{H}]^+{}^a$	1113.1	1112.9		×	×
$[\text{L} + 3\text{Cu} + 2\text{Cl} + 3\text{ClO}_4]^+$	1146.0	1146.0			×
$[\text{L} + 3\text{Cu} + \text{Cl} + 4\text{ClO}_4]^+$	1210.0	1209.9			×
$[\text{L} + 3\text{Cu} + 5\text{ClO}_4]^+$	1274.0	1273.7			×

<sup>a</sup> In these species at least one copper is as  $\text{Cu}^+$ .

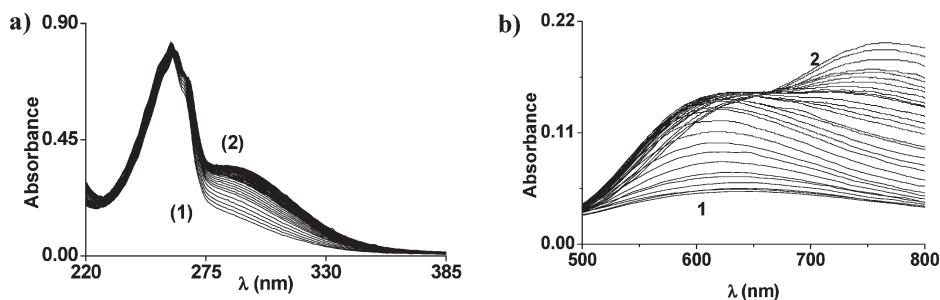


**Figure 4.** UV-vis spectra of the system  $\text{Cu}^{2+}/\text{L}^1$  (1:1) recorded as a function of  $\text{p}[\text{H}]$ . Solvent:  $\text{H}_2\text{O}$ ;  $I = 0.15 \text{ mol dm}^{-3}$  ( $\text{NaClO}_4$ );  $T = 298.1(1) \text{ K}$ . (a)  $l = 1 \text{ cm}$ ;  $[\text{L}^1]_{\text{tot}} = 6.22 \times 10^{-5} \text{ mol dm}^{-3}$ ; (1)  $\text{p}[\text{H}] = 3.69$ ; (2)  $\text{p}[\text{H}] = 9.52$ . (b)  $l = 1 \text{ cm}$ ;  $[\text{L}^1]_{\text{tot}} = 9.20 \times 10^{-4} \text{ mol dm}^{-3}$ ; (1)  $\text{p}[\text{H}] = 2.45$ ; (2)  $\text{p}[\text{H}] = 9.58$ .

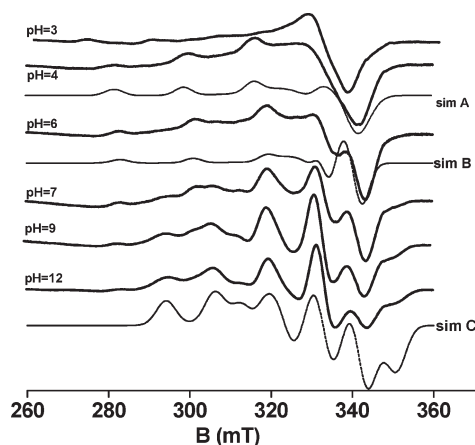


**Figure 5.** EPR spectra of frozen solutions at different  $\text{p}[\text{H}]$  of the complex  $\text{CuL}^1$ , together with computer simulated spectra. sim A ( $\text{p}[\text{H}] = 4.0$ ); sim B ( $\text{p}[\text{H}] = 6.0$ ); sim C ( $\text{p}[\text{H}] = 12.0$ ). Solvent: water/glycol (70/30 v/v);  $T = 77 \text{ K}$ ;  $[\text{L}^1]_{\text{tot}} = 3 \times 10^{-3} \text{ mol dm}^{-3}$ ;  $[\text{Cu}^{2+}]_{\text{tot}}/[\text{L}^1]_{\text{tot}} = 1.0$ .

**Table 4.** Spectral Parameters of the Mononuclear  $\text{Cu}^{2+}\text{-L}^1$  Complexes and of the Trinuclear  $\text{Cu}_3\text{L}^1$  Species

species <sup>a</sup>	$\lambda_{\text{max}}(\text{nm})^b$	$\epsilon_{\text{max}}(\times 10^3 \text{ mol}^{-1} \text{ dm}^3 \text{ cm}^{-1})$
$\text{CuH}_2\text{L}^1$	762	0.22
	633	0.161
	260	13.0
$\text{CuH}_3\text{L}^1$	288	5.6
	623	0.173
	259	14.2
$\text{CuH}_4\text{L}^1$	288	4.1
	620	0.116
$\text{Cu}_3\text{L}^1$	257	25.2(1)
	280	10.9(5)
	627	0.39(2)

<sup>a</sup> Charges are omitted for the sake of clarity. <sup>b</sup>  $\lambda$  values are provided with  $\pm 2 \text{ nm}$  accuracy and the  $\epsilon$  values with 5% error.

downfield changes in their chemical shift.<sup>23</sup> Therefore, to obtain further information about the protonation sequence of our compounds we have recorded the  $^1\text{H}$  NMR and  $^{13}\text{C}$  NMR of  $\text{L}^1$  versus  $\text{p}[\text{D}]$ . Below  $\text{p}[\text{D}] = 3.0$  important downfield shifts are observed for the signals of all the aromatic protons of the pyridines supporting that at this stage the pyridine nitrogens are protonated. Moreover, the singlet signal 8, attributed to the protons closest to these pyridine rings (for the labeling see Chart 1), is also significantly downfield shifted below this  $\text{p}[\text{D}]$  (Figure 2). These data support again the protonation of the pyridine units below  $\text{p}[\text{H}] = 3$ .

The low value of the protonation constant of the pyridine groups and a comparison with corresponding values obtained for various aminopyridine ligands,<sup>24,25</sup> suggest that protonation of the pyridine ring implies the breakage of hydrogen bonds (Chart 2) formed with the vicinal amino groups.<sup>27–29</sup> As already reported for the tripodal polyamine *tren*, the apical nitrogen atom would not bear any neat protonation throughout all the studied pH range.<sup>30</sup>

**$\text{Cu}^{2+}$  Complexation Equilibria.** The stability constants related to the formation in aqueous solution of mono-, di-, and trinuclear complexes of the polyamine  $\text{L}^1$  are shown in Table 2 along with the constants previously reported for the precursor polyamine  $\text{L}^2$ .<sup>11</sup> All these constants have been obtained at 298.1(1) K in  $0.15 \text{ mol dm}^{-3}$   $\text{NaClO}_4$ . In the titrations carried out for  $\text{Cu}^{2+}/\text{L}^1$  3:1 molar ratio, the  $\text{p}[\text{H}]$  range covered was 2.0–6.0 because of the occurrence of precipitation at higher  $\text{p}[\text{H}]$  values.

$\text{L}^1$  forms in aqueous solution mononuclear species of  $[\text{CuH}_r\text{L}]^{(2+r)+}$  stoichiometry with  $r$  varying between 0 and 4. These species are predominant at molar ratios  $\text{Cu}^{2+}/\text{L}^1$  lower than 1:1 (Figure 3a). For a higher  $\text{Cu}^{2+}/\text{L}^1$  ratio, the dinuclear species  $[\text{Cu}_2\text{L}]^{4+}$ ,  $[\text{Cu}_2\text{HL}]^{5+}$ , and  $[\text{Cu}_2\text{L}(\text{OH})_2]^{2+}$  and the trinuclear ones  $[\text{Cu}_3\text{L}]^{6+}$  and  $[\text{Cu}_3\text{HL}]^{7+}$  are also observed (see the distribution diagrams in Figure 3, panels b and c). The nuclearity of these copper(II) species has been confirmed by the ESI/MS<sup>+</sup> method (Table 3 and Supporting Information, Figure S3).

**Mononuclear Complexes.** The 10 nitrogen donors in  $\text{L}^1$  can be classified into 3 categories: (i) the secondary amino groups of the arms, (ii) the apical tertiary nitrogen atom, and (iii) the pyridine nitrogen atoms. This number exceeds by far the preferred coordination number of  $\text{Cu}^{2+}$  and thereby, it is interesting to know how many and which are the nitrogen atoms involved in the coordination of the different mononuclear complexes. Although it is difficult to establish coordination numbers just from the free energy terms, the number of protonated species and the values of their formation and stepwise protonation constants give some valuable indication in this respect. First, the value of the stability constant of  $[\text{CuL}^1]^{2+}$  is

- (27) Chmielewski, M.; Jurczak, J. *Chem.—Eur. J.* **2005**, *11*, 6080–6094.  
 (28) Hossain, Md. A.; Kang, S. O.; Powell, D.; Bowman-James, K. *Inorg. Chem.* **2003**, *42*, 1397–1399.  
 (29) (a) Lacoste, R. G.; Martell, A. E. *Inorg. Chem.* **1964**, *3*, 881–884.  
 (b) Goldberg, D. E.; Femelius, W. C. *J. Phys. Chem.* **1959**, *63*, 1246–1249.  
 (c) Mayer, J. M.; Testa, B. *Helv. Chim. Acta* **1982**, *65*, 1868–1884.  
 (30) Thaler, F.; Hubbard, C. D.; Heinemann, F. W.; van Eldik, R.; Schindler, S.; Fabian, I.; Dittler-Klingemann, A. M.; Hahn, F. E.; Orvig, C. *Inorg. Chem.* **1998**, *37*, 4022–4029.

**Table 5.** EPR Parameters of the Different Mononuclear Species Existing in the System  $\text{Cu}^{2+}\text{-L}^1$ 

species		$g_{zz}$	$g_{xx}$	$g_{yy}$	$A_{zz}$ ( $10^{-4}$ cm $^{-1}$ )	$A_{xx}$ ( $10^{-4}$ cm $^{-1}$ )	$A_{yy}$ ( $10^{-4}$ cm $^{-1}$ )
$\text{CuH}_4\text{L}^{1a}$	simA	2.223	2.089	2.050	174	49	24
$\text{CuH}_3\text{L}^1$	simB	2.206	2.065	2.050	182	40	24
$\text{CuH}_2\text{L}^1$	simC	$g_1 = 2.009$	$g_2 = 2.082$	$G_3 = 2.189$	66	85	119

<sup>a</sup> Charges are omitted for the sake of clarity.

**Table 6.** Cumulative Stability Constants for the Mono-, Di-, and Trinuclear Copper Complexes of the Ligand  $\text{L}^1$ -Copper(II) Species Determined from the Spectrophotometric vs p[H] Data and from the Potentiometric Data<sup>a</sup>

reaction	$\log \beta$ ( $3\sigma$ ) <sup>b</sup>	$\log \beta$ ( $3\sigma$ ) <sup>c</sup>
$\text{Cu}^{2+} + 2\text{H}^+ + \text{L}^1 \rightleftharpoons [\text{CuH}_2\text{L}^1]^{4+}$	35.4(2)	36.8(1)
$\text{Cu}^{2+} + 3\text{H}^+ + \text{L}^1 \rightleftharpoons [\text{CuH}_3\text{L}^1]^{5+}$	42.2(4)	42.34(9)
$\text{Cu}^{2+} + 4\text{H}^+ + \text{L}^1 \rightleftharpoons [\text{CuH}_4\text{L}^1]^{6+}$	46.8(3)	46.58(9)
$2\text{Cu}^{2+} + \text{H}^+ + \text{L}^1 \rightleftharpoons [\text{Cu}_2\text{HL}^1]^{5+}$	39.6(3)	38.2(2)
$3\text{Cu}^{2+} + \text{L}^1 \rightleftharpoons [\text{Cu}_3\text{L}^1]^{6+}$	38.9(1)	38.3(1)

<sup>a</sup>  $I = 0.15$  mol dm $^{-3}$  (NaClO $_4$ );  $T = 298.1(1)$  K). <sup>b</sup> Spectrophotometric vs p[H] titrations. <sup>c</sup> Potentiometric titrations.

only slightly lower than that of  $[\text{CuL}^2]^{2+}$  (entry 1, Table 2), for which a coordination number of five was inferred.<sup>11</sup> Second, the stability constant of the complex with  $\text{L}^1$  is higher than that reported for the analogous complex with the parent polyamine *tren* ( $\log K = 19.58$ )<sup>1,25,30</sup> which displays a trigonal bipyramidal geometry with the involvement in the first coordination sphere of all its four nitrogen atoms and an additional exogen ligand.<sup>31</sup> Third, the constants for the first two protonation steps of the complex  $[\text{CuL}^1]^{2+} + \text{H}^+ \rightleftharpoons [\text{CuHL}^1]^{3+}$  and  $[\text{CuHL}^1]^{3+} + \text{H}^+ \rightleftharpoons [\text{CuH}_2\text{L}^1]^{4+}$  (Table 2) are high and compare quite well with the constants of the third and fourth protonation steps of the free ligand displaying the same overall charges  $[\text{H}_2\text{L}^1]^{2+} + \text{H}^+ \rightleftharpoons [\text{H}_3\text{L}^1]^{3+}$ ,  $\log K = 8.54$  and  $[\text{H}_3\text{L}^1]^{3+} + \text{H}^+ \rightleftharpoons [\text{H}_4\text{L}^1]^{4+}$ ,  $\log K = 7.54$ , respectively (Table 1). These observations strongly suggest that the protonation step occurs on nitrogen atoms not directly bound to the  $\text{Cu}^{2+}$  ion and that at most five nitrogen atoms of the tripod would be involved in the coordination sphere of  $[\text{CuL}^1]^{2+}$ ,  $[\text{CuHL}^1]^{3+}$ , and  $[\text{CuH}_2\text{L}^1]^{4+}$  complexes. The third and fourth protonation steps of the metal complexes have protonation constants which are significantly lower (entries 4 and 5 in Table 2) than the corresponding ones of the free ligand (entries 5 and 6 in Table 1). The lowering of these protonation constants in the copper(II) complex with respect to the corresponding ones in the free ligand indicates that these nitrogen atoms are most likely involved in the coordination of  $\text{Cu}^{2+}$ .

To get more information about coordination numbers and geometries of the mononuclear complexes, we have recorded the variation with the p[H] of the UV–vis and EPR spectra of solutions containing equimolar amounts of  $\text{Cu}^{2+}$  and  $\text{L}^1$  (Figure 4 and 5 and Tables 4 and 5, respectively).

The spectrum in the UV domain consists, at the acidic p[H] values where  $[\text{CuH}_4\text{L}^1]^{6+}$  predominates, of an absorption band centered at about 259 nm attributable to a  $\pi\text{-}\pi^*$  transition of the pyridines,<sup>26</sup> followed by a shoulder at around 288 nm that can be ascribed to a ligand to  $\text{Cu}^{2+}$  charge transfer band (amino-to- $\text{Cu}^{2+}$

CT) (Figure 4a and Table 4).<sup>32</sup> In the visible region a broadband centered at 623 nm is observed (Figure 4b, Table 4) easily attributable to the less absorptive  $d_{xz}$ ,  $d_{xy}$ – $d_{z^2}$  transitions.<sup>33</sup> The EPR spectrum of this species shows a characteristic axial feature (Figure 5) corresponding to small rhombic distortion of a square pyramidal geometry (Table 5).

When the p[H] was raised to the values for which the triprotonated  $[\text{CuH}_3\text{L}^1]^{5+}$  species predominates in solution (p[H] ca. 5.0, Figure 3a), the intensity of all the bands increases without changing their shape and position. The EPR spectrum does not change significantly, its parameters with small rhombic character are also characteristic of a slightly distorted square pyramidal geometry (Table 5). Further addition of base to form  $[\text{CuH}_2\text{L}^1]^{4+}$  species produces, however, sharp changes in the d-d band and in the EPR spectrum. Indeed, while the changes in the UV region are not significant, the d-d band appears now as a shoulder at 633 nm, which experiences a bathochromic shift to 762 nm ( $9 < \text{p[H]} < 4.5$ ) in agreement with a coordination geometry close to trigonal bipyramid.<sup>34</sup> The EPR spectrum exhibits significant rhombicity of  $g$  and  $A$  parameters (Table 5, Figure 5) and “reverse” character, revealed in particular by a  $g_1$  parameter very close to the free electron value, supporting<sup>35,36</sup> a geometry strongly shifted toward the trigonal bipyramid for  $[\text{CuH}_2\text{L}^1]^{4+}$ .

Interestingly, such structural transformations were not observed in the EPR spectra in the case of  $\text{L}^2$ ,<sup>11</sup> although the UV–vis spectra of this polyamine showed features of trigonal bipyramidal geometry throughout all the p[H] range of complex formation.

Upon addition of further equivalents of base (pH > 7) neither the UV–vis nor the EPR spectra experienced further significant changes, supporting that the coordination sphere around the metal ion is the same in  $[\text{CuH}_2\text{L}^1]^{4+}$ ,  $[\text{CuHL}^1]^{3+}$ , and  $[\text{CuL}^1]^{2+}$ .

By using the SPECFIT<sup>19</sup> program it has been possible to determine the formation constants for the  $[\text{CuH}_4\text{L}^1]^{6+}$ ,  $[\text{CuH}_3\text{L}^1]^{5+}$ , and  $[\text{CuH}_2\text{L}^1]^{4+}$  species (Table 6) that are in reasonable agreement with the values derived from the potentiometric curves. The calculated UV–vis spectra for these species are collected in Supporting Information, Figure S4.

Taking into account the protonation sequence of the free ligand and all the thermodynamic and spectroscopic data of the mononuclear complex, the structural models

(32) Wei, N.; Murthy, N. N.; Karlin, D. K. *Inorg. Chem.* **1994**, *33*, 6093–6100.

(33) Hartam, J. R.; Vachet, R. W.; Pearson, W.; Wheat, R. J.; Callahan, J. H. *Inorg. Chim. Acta* **2003**, *343*, 119–132.

(34) McLachlan, G. A.; Fallon, G. D.; Martin, R. L.; Spiccia, L. *Inorg. Chem.* **1995**, *34*, 254–261.

(35) Addison, A. W.; Hendriks, H. M. J.; Reedijk, J.; Thompson, L. K. *Inorg. Chem.* **1981**, *20*, 103–110.

(36) Jitsukawa, K.; Harata, M.; Arii, H.; Sakurai, H.; Masuda, H. *Inorg. Chim. Acta* **2001**, *324*, 108–116.

(31) Laskowski, E. J.; Duggan, D. M.; Hendrickson, D. N. *Inorg. Chem.* **1975**, *14*, 2449–2459.

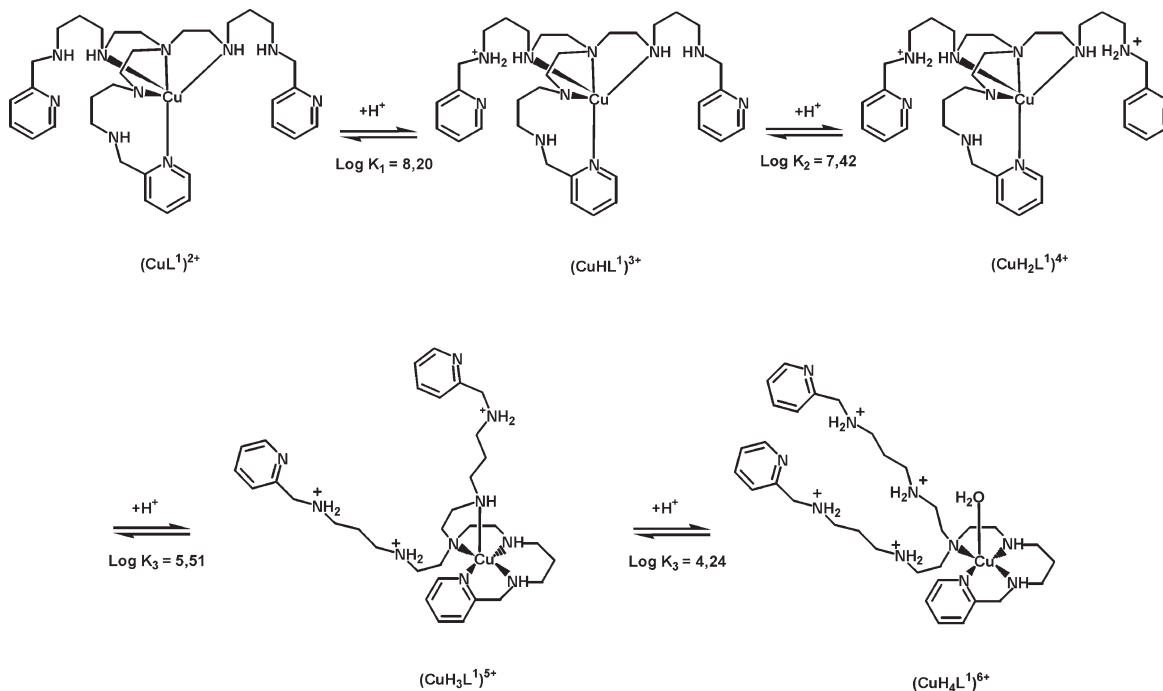


Figure 6. Protonation scheme of the  $[\text{CuL}^1]^{2+}$  species.

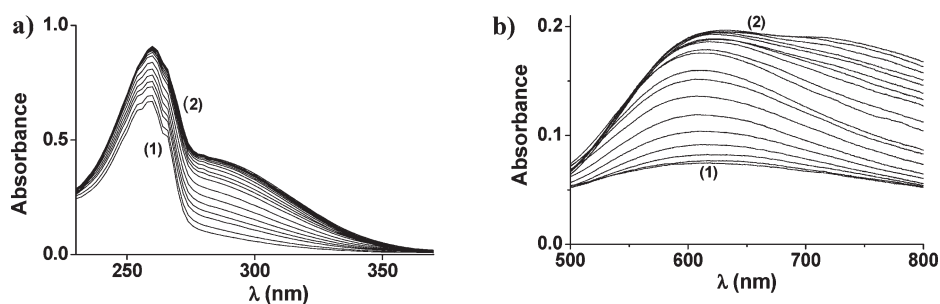


Figure 7. Spectrophotometric titration of the system  $\text{Cu}^{2+}\text{-L}^1$  in 2:1 molar ratio as a function of  $\text{p}[\text{H}]$ . Solvent:  $\text{H}_2\text{O}$ ;  $I = 0.15 \text{ mol dm}^{-3}$  ( $\text{NaClO}_4$ );  $T = 298.1(1) \text{ K}$ . (a)  $l = 1 \text{ cm}$ ;  $[\text{L}^1]_{\text{tot}} = 4.74 \times 10^{-5} \text{ mol dm}^{-3}$ ;  $[\text{Cu}^{2+}]_{\text{tot}} = 9.36 \times 10^{-5} \text{ mol dm}^{-3}$ ; (1)  $\text{p}[\text{H}] = 3.17$ ; (2)  $\text{p}[\text{H}] = 6.86$ . (b)  $l = 2 \text{ cm}$ ;  $[\text{L}^1]_{\text{tot}} = 1.19 \times 10^{-3} \text{ mol dm}^{-3}$ ;  $[\text{Cu}^{2+}]_{\text{tot}} = 2.38 \times 10^{-3} \text{ mol dm}^{-3}$ ; (1)  $\text{p}[\text{H}] = 2.60$ ; (2)  $\text{p}[\text{H}] = 6.18$ .

sketched in Figure 6 can be proposed. In the highest protonated species, the coordination will occur through one pyridine nitrogen atom, the apical nitrogen atom, and two secondary amino groups of one of the arms. This partial involvement of the arms of a tripodal ligand in metal binding has also been evidenced in the crystal structure of the monoprotonated  $\text{Cu}^{2+}$  complex of a related ligand in which the polyamine *tren* had been functionalized with 2-picolyl groups at the end of its three arms.<sup>37</sup> For the less protonated species (protonation degrees two and less), although other alternatives might be possible, a likely structure would involve the coordination of a secondary amino group of every arm apart from that of the apical and pyridine nitrogens.

**Di- and Trinuclear Complexes.** The  $[\text{Cu}_2\text{L}^1]^{4+}$  species is more stable than the analogous one formed with  $\text{L}^2$ . Indeed, addition of the second  $\text{Cu}^{2+}$  cation to  $[\text{CuL}^1]^{2+}$  to yield  $[\text{Cu}_2\text{L}^1]^{4+}$  is characterized by a successive stability constant which is about 3 orders of magnitude higher than the corresponding one with the polyamine  $\text{L}^2$  (entry 6 in

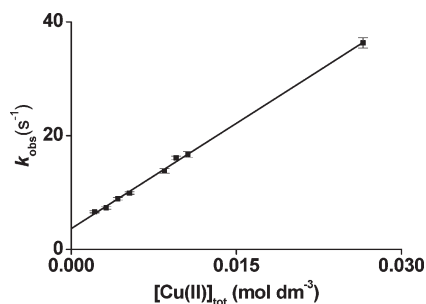
Table 2) suggesting that a much higher number of coordinating nitrogen atoms participate in the binding of the second metal ion. This is further confirmed by the possibility of leading to trinuclear complexes with a successive stability constant for the addition of the third  $\text{Cu}^{2+}$  cation equal to 6.6 logarithmic units (entry 9 in Table 2).

The spectrophotometric titration recorded in the UV and vis regions for  $\text{Cu}^{2+}/\text{L}^1$  systems in 2:1 and 3:1 molar ratios are shown in Figure 7 and Supporting Information, Figure S6, respectively. The spectra show, on going from  $\text{p}[\text{H}] = 3$ , where the tetraprotonated mononuclear species predominates, to  $\text{p}[\text{H}] = 6.2$ , where the species  $[\text{Cu}_2\text{HL}^1]^{5+}$  is formed, an increase in the molar absorptivity of the band at 259 nm as well as an increase in intensity of the band at 620 nm followed by the appearance of a shoulder at higher wavelengths although this change is not so evident as for molar ratios 1:1. No further changes<sup>38</sup> were observed at higher  $\text{p}[\text{H}]$  values ( $6.2 < \text{pH} < 9\text{--}10$ ). The increase in the absorptivity of the band centered at 259 nm suggests the involvement

(37) Gérard, C.; Mohamadou, A.; Marrot, J.; Brandes, S.; Tabard, A. *Helv. Chim. Acta* **2005**, *88*, 2397–2412.

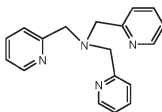
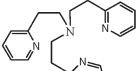
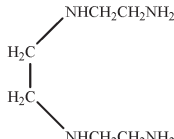
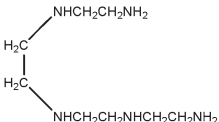
(38) Prenesti, E.; Daniele, P. G.; Prencipe, M.; Ostacoli, G. *Polyhedron* **1999**, *18*, 3233–3241.





**Figure 8.** Variation of the pseudo-first order rate constant ( $k_{\text{obs}}$ ) vs  $[\text{Cu(II)}]_{\text{tot}}$ . Solvent:  $\text{H}_2\text{O}$ ;  $\text{p}[\text{H}] = 2.39$ ;  $\lambda = 600 \text{ nm}$ ;  $T = 298.1(1) \text{ K}$ ;  $[\text{L}^1]_{\text{tot}} = 2.1 \times 10^{-4} \text{ mol dm}^{-3}$ .

**Table 7.** Rate Constants for the Formation of  $\text{Cu}^{2+}$  Complexes with Different Amines

Ligands	$k_f (\text{mol}^{-1} \text{ dm}^3 \text{ s}^{-1})^d$
$[\text{H}_6\text{L}^1]^{6+}$	$1.23 \times 10^3$
 HTPMA <sup>+(a)</sup>	$\sim 2 \times 10^7$
 TPEA <sup>(a)</sup> HTPEA <sup>+(a)</sup>	$\sim 3 \times 10^8$ $7.1 \times 10^5$
$\text{NH}_3^b$	$1.08 \times 10^5$
 H <sub>2</sub> TRIEN <sup>2+(c)</sup> H <sub>3</sub> TRIEN <sup>3+(c)</sup>	$7.5 \times 10^6$ $1.6 \times 10^4$
 H <sub>3</sub> TETREN <sup>3+(c)</sup> H <sub>4</sub> TETREN <sup>4+(c)</sup>	$9 \times 10^4$ $3.3 \times 10^4$

<sup>a</sup>Taken from ref 46. <sup>b</sup>Taken from ref 47. <sup>c</sup>Taken from ref 48. <sup>d</sup>Solvent:  $\text{H}_2\text{O}$ ,  $I = 0.15 \text{ mol dm}^{-3}$  ( $\text{NaClO}_4$ );  $T = 298.1(1) \text{ K}$ .

in the coordination sphere of the metal ion of a further pyridine nitrogen atom, while the shape of the d-d transitions at higher  $\text{p}[\text{H}]$  values suggests mixtures of bipyramidal trigonal and square pyramidal geometries.<sup>34</sup> Unfortunately, the EPR spectra for the dinuclear species are not very informative. The EPR data at  $\text{p}[\text{H}] = 2.0$  are similar to those previously commented for the tetraprotonated mononuclear species. At higher  $\text{p}[\text{H}]$  values, the EPR spectra revealed a badly resolved hyperfine structure due to spin–spin interaction between the copper(II) ions that is more evident at  $\text{p}[\text{H}]$  values about 10.

**Table 8.** Apparent Stability Constants for the Formation of  $\text{Cu}^{2+}$  Complexes of  $\text{L}^1$  Measured by Spectrophotometry in Water at  $\text{p}[\text{H}] = 5.45$ ,  $I = 0.1 \text{ mol dm}^{-3}$  (MES),  $T = 298.1(1) \text{ K}$

equilibria <sup>a,b</sup>	$\log K^* (3\sigma)$	
	experimental	calculated
$\text{Cu} + \text{L}^{1'} \rightleftharpoons \text{CuL}^{1'}$	8.1(9)	9.9
$\text{CuL}^{1'} + \text{Cu} \rightleftharpoons \text{Cu}_2\text{L}^{1'}$	7(1)	6.5
$\text{Cu}_2\text{L}^{1'} + \text{Cu} \rightleftharpoons \text{Cu}_3\text{L}^{1'}$	7(1)	5.6

<sup>a</sup>Charges are omitted for the sake of clarity. <sup>b</sup> $\text{L}^{1'}$  stands for the ligand without defining its actual protonation degree.

From the UV–vis spectral variations it has been possible to calculate the electronic spectrum of the species (Supporting Information, Figure S7) as well as its equilibrium constant which was found to be in good agreement with the value obtained from the potentiometric titrations.

The distribution diagram in Figure 3c shows that for  $\text{Cu}^{2+}/\text{L}^1$  3:1 molar ratio the trinuclear species predominates from  $\text{p}[\text{H}]$  about 4.5. At higher  $\text{p}[\text{H}]$  values some precipitation prevented one to observe the formation of hydroxylated species. The electronic spectra in the UV region shows upon addition of the third  $\text{Cu}^{2+}$  a further increase of the molar absorptivity of the band at 258 nm, again suggesting the involvement of a new pyridine nitrogen in the coordination of the  $\text{Cu}^{2+}$  cations. The spectra recorded in the visible region show a band centered at 627 nm that increases in intensity on raising the  $\text{p}[\text{H}]$ . However, there is not any clear indication of the formation of species with trigonal pyramidal geometry. The analysis of these data allowed to calculate the electronic spectrum of  $[\text{Cu}_3\text{L}^1]^6$  (Supporting Information, Figure S8 and Table 4).

### Formation Kinetics

**Kinetic Studies at  $\text{p}[\text{H}] = 2.39$ .** The formation kinetic studies were carried out using stopped flow spectrophotometry at two  $\text{p}[\text{H}]$  values (2.39 and 5.45). We have performed an absorption spectrophotometric titration of  $\text{L}^1$  ( $4.2 \times 10^{-4} \text{ mol dm}^{-3}$ ) by  $\text{Cu}^{2+}$  at  $\text{p}[\text{H}]$  2.39 ( $0 < [\text{Cu}^{2+}]_{\text{tot}}/[\text{L}^1]_{\text{tot}} < 5.43$ ). The spectral variations of the  $\text{Cu}^{2+}$  centered d-d bands (Supporting Information, Figure S9a) were monitored and the statistical processing<sup>19</sup> of the corresponding absorption data allowed characterizing a single monocopper(II) species. Its stability constant at  $\text{pH}$  2.39 was calculated to be  $\log K^*_{\text{CuL}^1} = 2.7(6)$  and is in agreement with the recalculated one<sup>39</sup> (see Supporting Information for further information) from data of Table 2 ( $\log K^*_{\text{CuL}^1} = 3.06$ ). Moreover, it is noteworthy that the corresponding distribution diagrams (Figure 3a) show that the  $[\text{CuH}_4\text{L}^1]^{6+}$  is the major species at  $\text{p}[\text{H}]$  2.39. Pseudo-first order conditions were chosen to carry out formation kinetics. Absorbance at  $\lambda = 600 \text{ nm}$  (Supporting Information, Figure S10) experiences an exponential variation versus time indicating a first order formation

(39) Ringbom, A. *Les complexes en chimie analytique*; Dunod: France, 1967; p 369. Schwarzenbach, G.; Flaschka, H. *Complexometric Titrations*; Methuen: London, 1969, p 114.

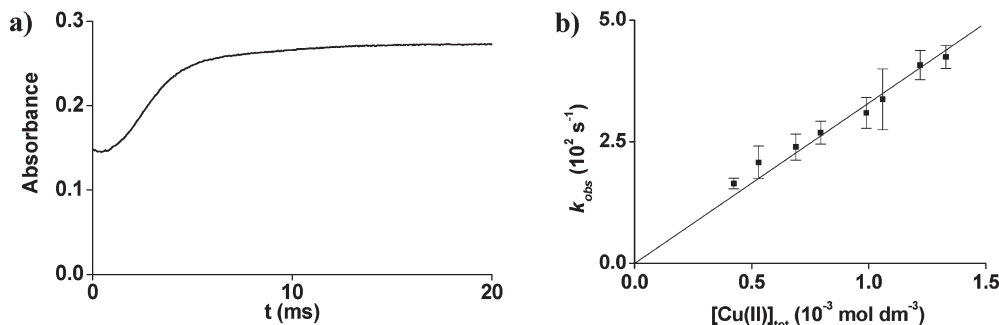


**Figure 9.** (a) Variation of the absorbance vs time for the formation of copper(II) complex with  $L^1$  in excess of  $[Cu^{2+}]_{tot}$  at p[H] 5.45. Solvent:  $H_2O$ ; p[H] = 5.45 ( $0.1 \text{ mol dm}^{-3}$  MES);  $T = 298.1(1) \text{ K}$ ;  $[L^1]_{tot} = 2.31 \times 10^{-5} \text{ mol dm}^{-3}$ . (a)  $[Cu^{2+}]_{tot}/[L^1]_{tot} = 34.41$ ,  $l = 1 \text{ cm}$ ;  $\lambda = 285 \text{ nm}$ . (b) Variation of the pseudo-first order rate constant ( $k_{obs}$ ) vs  $[Cu^{2+}]_{tot}$ .

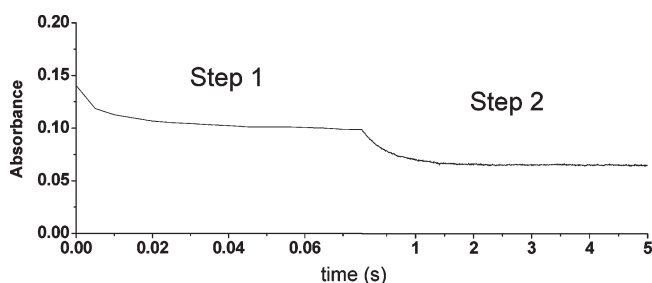


**Figure 10.** Spectral absorption changes vs time for the acid-induced dissociation of the complex  $CuL^1$ . Solvent:  $H_2O$ ;  $l = 0.15 \text{ mol dm}^{-3}$  ( $NaClO_4$ );  $l = 1 \text{ cm}$ ;  $[CuL^1]_{tot} = 4.39 \times 10^{-5} \text{ mol dm}^{-3}$ ;  $[H^+]_{tot} = 1.11 \times 10^{-3} \text{ mol dm}^{-3}$ ;  $T = 298.1(1) \text{ K}$ ;  $\lambda = 285 \text{ nm}$ .

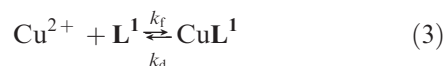
kinetics with respect to the ligand:

$$v = -d[L^1]/dt = k_{obs}[L^1] \quad (1)$$

No fast steps could be evidenced during the mixing time ( $\sim 3 \text{ ms}$ ) of the stopped-flow device. Moreover, the absorbance at the end of the rate limiting step satisfactorily corresponds to the expected absorbance value. The pseudo-first order rate constants  $k_{obs}$  ( $s^{-1}$ ) were determined for various  $Cu^{2+}$  concentrations (Supporting Information, Table S1). A linear dependence of  $k_{obs}$  on  $Cu^{2+}$  analytical concentrations was observed (Figure 8) in agreement with the following relationship:

$$k_{obs} = k_f[Cu^{2+}]_{tot} + k_d \quad (2)$$

This equation corresponds to the equilibrium



The values of  $k_f$  and  $k_d$  were calculated to be  $1.23(5) \times 10^3 \text{ mol}^{-1} \text{ dm}^3 \text{ s}^{-1}$  and  $3.7(6) \text{ s}^{-1}$ , respectively. The logarithmic value of the  $k_f/k_d$  ratio ( $2.5(2)$ ) agrees well with

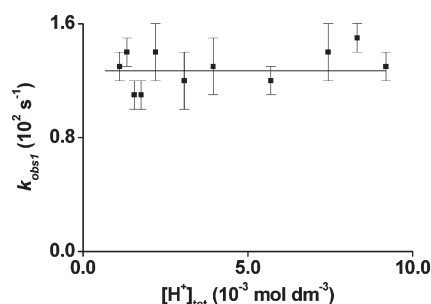
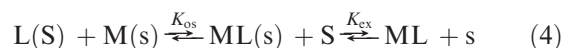


**Figure 11.** Variation of  $k_{obs1}$  rate constant vs  $[H^+]_{tot}$  for the acid-promoted dissociation of the mononuclear  $CuL^1$  complex.  $[CuL^1]_{tot} = 4.39 \times 10^{-5} \text{ mol dm}^{-3}$ ;  $T = 298.1(1) \text{ K}$ ;  $l = 0.15 \text{ mol dm}^{-3}$  ( $NaClO_4$ ).

the conditional stability constant obtained at p[H] 2.39 ( $\log K^*_{CuL^1} = 2.6(7)$ ), thus substantiating the proposed mechanism. Formation kinetics of metal complexes and, in particular, of copper(II) complexes<sup>40–46</sup> with a wide variety of ligands showed that these processes could follow a dissociative mechanism, which has been described by Eigen–Wilkins as follows:<sup>41–43</sup>



The rate limiting step corresponds to the desolvation of the metal in an outer-sphere complex formed in a fast pre-equilibrium (eq 5).

$$k_f = K_{os} \times k_{ex} \quad \text{with} \quad k_f(\text{mol}^{-1} \text{ dm}^3 \text{ s}^{-1}), \\ K_{os}(\text{mol}^{-1} \text{ dm}^3), k_{ex}(\text{s}^{-1}) \quad (5)$$

Using  $K_{os}^{48,44}$  ( $1.6 \times 10^{-5} \text{ mol}^{-1} \text{ dm}^3$ ) for free ligand ( $[H_6L^1]^{6+}$ ) and  $Cu^{2+}$  as well as the reported  $k_{ex}$  value<sup>41,45</sup> ( $2 \times 10^8 \text{ s}^{-1}$ ) for the desolvation of the copper(II) cation, we calculated  $k_f = 3.2 \times 10^3 \text{ mol}^{-1} \text{ dm}^3 \text{ s}^{-1}$ . This value is of the same order as that obtained experimentally ( $k_f = 1.23(5) \times 10^3 \text{ mol}^{-1} \text{ dm}^3 \text{ s}^{-1}$ ), so it can be reasonably concluded that the formation of  $[CuH_4L^1]^{6+}$  proceeds through an Eigen–Wilkins mechanism.

(40) Palanché, T.; Blanc, S.; Hennard, C.; Abdallah, M. A.; Albrecht-Gary, A. M. *Inorg. Chem.* **2004**, *43*, 1137–1152. (b) Tomišić, V.; Blanc, S.; Elhabiri, M.; Expert, D.; Albrecht-Gary, A. M. *Inorg. Chem.* **2008**, *47*, 9419–9430. (c) Albrecht-Gary, A. M.; Blanc, S.; Rochel, N.; Ocaktan, A. Z.; Abdallah, M. A. *Inorg. Chem.* **1994**, *33*, 6391–6402. (d) Albrecht-Gary, A. M.; Crumbliss, A. L. *Metal Ions in Biological Systems*; Sigel, A., Sigel, H., Eds.; Marcel Dekker: New York, 1998; Vol. 35, pp 239–327. (e) Albrecht-Gary, A. M.; Crumbliss, A. L. *Scientific Bridges for 2000 and Beyond*, TEC and DOC eds.; Institut de France, Académie des Sciences: Paris, 1999; pp 73–89.

(41) Roche, T. S.; Wilkins, R. G. *J. Am. Chem. Soc.* **1974**, *96*, 5082–5086.

(42) Eigen, M.; Wilkins, R. G. *Adv. Chem. Ser.* **1965**, *49*, 55–67.

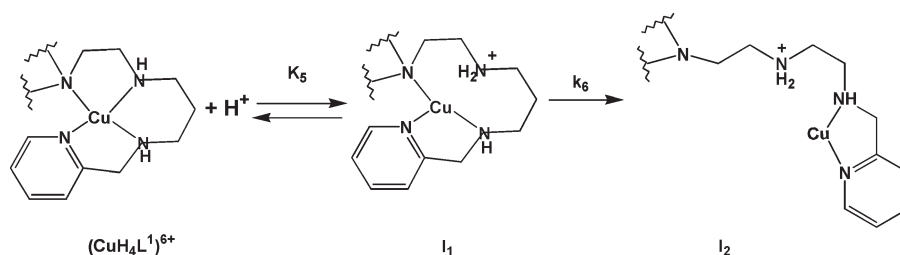
(43) Eigen, M. *Pure Appl. Chem.* **1963**, *6*, 97–115.

(44) Fuoss, R. M. *J. Am. Chem. Soc.* **1958**, *80*, 5059–5061.

(45) Diebler, H.; Eigen, M.; Ilgenfritz, G.; Maab, G.; Winkler, R. *Pure Appl. Chem.* **1969**, *20*, 93–115.

(46) Ambundo, E. A.; Deydier, M.-V.; Ochymowycz, L. A.; Rorabacher, D. B. *Inorg. Chem.* **2000**, *39*, 1171–1179.

Chart 3



The bimolecular rate constant  $k_f$  for the formation of  $[\text{CuH}_4\text{L}^1]^{6+}$  is much lower than those reported for other polyamine ligands (Table 7). This can be mainly ascribed to the high positive charge of  $[\text{H}_6\text{L}^1]^{6+}$ , which decreases the formation rates with the divalent copper(II) cation. Depending on the  $\text{p}[\text{H}]$  and on the number of the protonation sites, the differences could reach several orders of magnitude, as shown in Table 7.

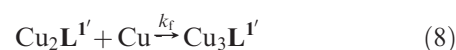
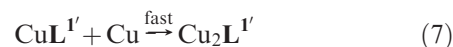
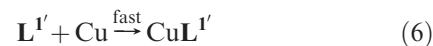
**Kinetic Studies at  $\text{p}[\text{H}] = 5.45$ .** Conditional thermodynamic constants for  $\text{Cu}^{2+}$  complexes, determined by absorption spectrophotometry (Supporting Information, Figure S9b), are presented in Table 8. At  $\text{p}[\text{H}] 5.45$ , the major species of free ligand is  $[\text{H}_6\text{L}^1]^{6+}$  (Supporting Information, Figure S1) and the trinuclear complex  $\text{Cu}_3\text{L}^1$  dominates in excess of copper(II) (Supporting Information, Figure S11).

The kinetic experiments were monitored under pseudo-first order conditions with respect to the metal and at  $\lambda = 285 \text{ nm}$ , which corresponds to the ligand-to-metal charge transfer band (Figure 4). Significant loss of spectrophotometric amplitude was observed during the mixing time of the reactants because of the occurrence of fast reactions, which are not accessible on the time scale of the stopped-flow technique ( $\sim 3 \text{ ms}$ ). An exponential signal was observed in the millisecond time span (Figure 9a). The absorbance at the end of this rate limiting step is in good agreement with the value expected thus indicating that no slower steps take place.

Pseudo-first order rate constants  $k_{\text{obs}}$  ( $\text{s}^{-1}$ ) were determined (Supporting Information, Table S2). They linearly vary with  $[\text{Cu}^{2+}]_{\text{tot}}$  without significant intercept at the origin (Figure 9b).

Taking into account the spectrophotometric observations and the thermodynamic data, we could suggest that the rate limiting step corresponds to the complexation of

the third  $\text{Cu}^{2+}$  cation, the formation of  $\text{CuL}^{1'}$  and  $\text{Cu}_2\text{L}^{1'}$  species being fast.



The rate law can therefore be written

$$v = d[\text{Cu}_3\text{L}^{1'}]/dt = k_f[\text{Cu}_2\text{L}^{1'}]_t[\text{Cu}]_t \quad (9)$$

and leads to the following relationship:

$$\begin{aligned} k_{\text{obs}} &= k_f[\text{Cu}]_{\text{tot}} \quad \text{with} \quad k_f \\ &= 3.30(7) \times 10^5 \text{ mol}^{-1} \text{ dm}^3 \text{ s}^{-1} \quad (10) \end{aligned}$$

Assuming a dissociative mechanism dependent on the desolvation of  $\text{Cu}^{2+}$ , we could estimate  $K_{\text{os}}^{44,47} = 4.6 \times 10^{-4} \text{ mol}^{-1} \text{ dm}^3$  and  $k_{\text{ex}} = 2 \times 10^8 \text{ s}^{-1}$  and deduce  $k_f = 9.2 \times 10^4 \text{ mol}^{-1} \text{ dm}^3 \text{ s}^{-1}$ . This value of the bimolecular rate constant is in good agreement with the experimental  $k_f$  value ( $3.3(7) \times 10^5 \text{ mol}^{-1} \text{ dm}^3 \text{ s}^{-1}$ ).

**Dissociation Kinetics.** The global dissociation reaction of the  $\text{CuL}^1$  under acidic conditions can be written:



The variation of the absorbance at  $\lambda = 285 \text{ nm}$  was monitored versus time in a range of  $\text{p}[\text{H}]$  between 3.0 and 2.0. A large spectrophotometric amplitude was lost during the mixing time of the stopped-flow instrument. This suggests that very fast reactions, not accessible under our experimental conditions, occur and involve the main chromophores. The absorbance after 3 ms corresponds to the tetraprotonated complex  $[\text{CuH}_4\text{L}^1]^{6+}$ . In addition, the kinetic recordings reveal two well separated rate limiting steps in the milliseconds and seconds time spans, respectively (Figure 10).

Both steps display exponential decay versus time. The values of the corresponding pseudo-first-order rate constants are reported in Supporting Information, Table S3.  $k_{\text{obs1}}$  is independent of the proton concentrations

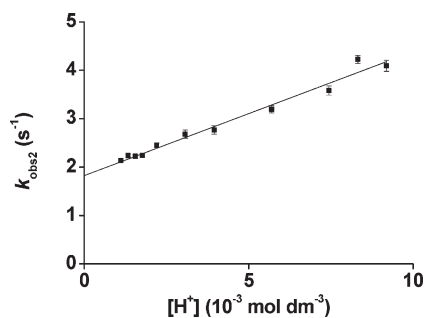


**Figure 12.** Variation of the  $k_{\text{obs2}}$  rate constant vs  $[\text{H}^+]_{\text{tot}}$  for the acid-promoted dissociation of the mononuclear  $\text{CuL}^1$  complex.  $[\text{CuL}^1]_{\text{tot}} = 4.39 \times 10^{-5} \text{ mol dm}^{-3}$ ;  $T = 298.1(1) \text{ K}$ ;  $I = 0.15 \text{ mol dm}^{-3}$  ( $\text{NaClO}_4$ ).

(47) Sokol, L. S.W. L.; Fink, T. D.; Rorabacher, D. B. *Inorg. Chem.* **1980**, *19*, 1263–1266.

(48) Moss, D. B.; Lin, C.-T.; Rorabacher, D. B. *J. Am. Chem. Soc.* **1973**, *95*, 5179–5185.

Chart 4

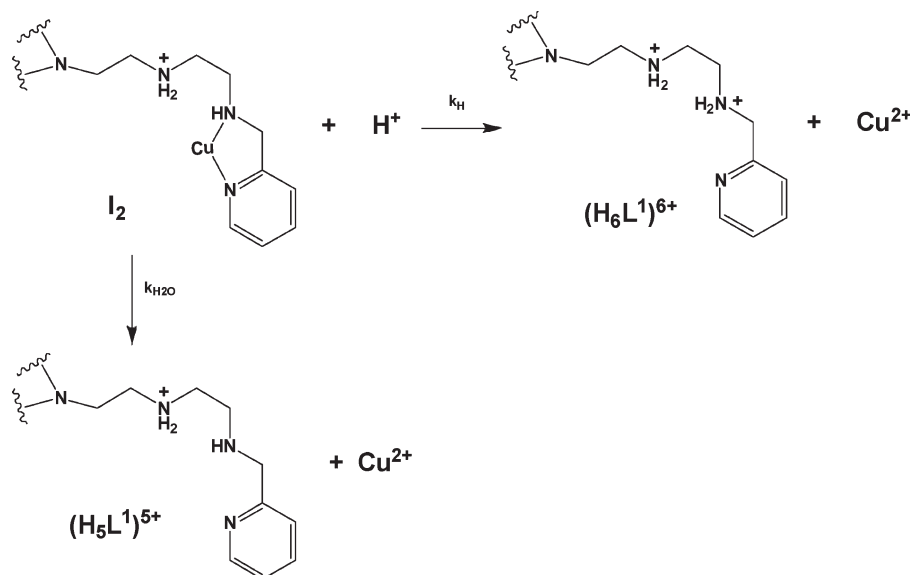


(Figure 11). Therefore, an averaged  $k_{obs1}$  value can be easily determined ( $1.32(8) \times 10^2 \text{ s}^{-1}$ ).

To rationalize our data relative to the first step, we suggest a saturation mechanism due to a protonation fast pre-equilibrium. The tetraprotonated  $[CuH_4L^1]^{6+}$  is indeed further protonated leading to kinetic intermediate  $I_1$  with a secondary amine vicinal to the anchor being protonated and dissociated from the metal. A rate limiting rearrangement of  $I_1$  to  $I_2$  corresponds to the dissociation of the Cu–N bond of the anchor (Chart 3).

This mechanism can be interpreted by the rate law given eq 12. Under our experimental conditions, the term  $K_5[H^+]$  is much higher than 1 so eq 12 can be simplified to eq 13:

$$k_{obs1} = \frac{k_6 K_5 [H^+]_{tot}}{1 + K_5 [H^+]_{tot}} \quad (12)$$

$$k_{obs1} = k_6 \quad (13)$$

The  $k_{obs2}$  values determined for the second rate limiting step fit a linear plot with respect to the  $H^+$  concentrations with a significant intercept at the origin (Figure 12).

In step 2, the complete dissociation of the copper(II) complex takes place (Chart 4). The dissociation occurs through two different pathways, the competitive attack of the protons and of the solvent.<sup>49–51</sup> In agreement with processes previously reported for  $Cu^{2+}$  complexes with various polyamines,<sup>52</sup> the kinetic data agree well with the following rate law:

$$k_{obs2} = k_H [H^+] + k_{H_2O} \quad (14)$$

with  $k_H = 2.6(1) \times 10^2 \text{ mol}^{-1} \text{ dm}^3 \text{ s}^{-1}$  and  $k_{H_2O} = 1.82(5) \text{ s}^{-1}$ .

The second step is much slower ( $\sim 2\text{--}5 \text{ s}$ ) than the first one ( $\sim 50 \text{ ms}$ ). This slowing down reflects the stability of the bidentate coordination site with both a pyridine nitrogen and a secondary amine bound to  $Cu^{2+}$ , as already reported elsewhere.<sup>53–56</sup>

The  $k_H/k_{H_2O}$  ratio provides information about the solvolysis and the acid-triggered dissociation of  $I_2$ . The calculation of  $k_H/k_{H_2O} = 1.43(9) \times 10^2 \text{ mol}^{-1} \text{ dm}^3$  shows that below pH 2 the proton-catalyzed pathway governs the decomposition of the copper(II) complex. The macrocyclic metal complexes are mostly efficiently dissociated via an acidic catalysis.<sup>57</sup> Electrostatic repulsions could also weaken the attack of protons compared to the solvent and so decrease the ratio  $k_H/k_{H_2O}$ . Moreover, the stabilization of the copper(II) species by a five chelate ring, as in  $I_2$ , explains the prevailing acidic pathway over the solvolysis process.<sup>50,51,56</sup>

## Conclusions

A tripod ligand ( $L^1$ ) derived from the polyamine *tren* by extending the three arms with aminopropyl groups and further functionalization of the terminal sites with 2-picolyl functions has been prepared in good yield following a straightforward synthetic route. The acido-basic properties of  $L^1$  have been determined and the protonated species have been characterized by absorption spectrophotometric and  $^1H$  NMR methods. In the presence of  $Cu^{2+}$ ,  $L^1$  is able to form mono-, di-, and trinuclear copper(II) complexes depending on  $p[H]$  and on  $Cu^{2+}/L$  molar ratio. Induced by the protonation state that the mononuclear  $L^1$  complexes experienced, a conformational rearrangement was clearly evidenced.

(53) Hay, R. W.; Hassan, M. M.; Fenton, D. E.; Murphy, B. P. *Trans. Met. Chem.* **1994**, *19*, 559–560.

(54) Sun, H.; Lin, H.; Zhu, S.; Zhao, G.; Su, X.; Chen, Y. *Polyhedron* **1999**, *18*, 1045–1048.

(55) Díaz, P.; Basallote, M. G.; Mañez, M. A.; García-España, E.; Gil, L.; Latorre, J.; Soriano, C.; Verdejo, B.; Luis, S. V. *J. Chem. Soc., Dalton Trans.* **2003**, 1186–1193.

(56) Liang, B. F.; Chung, C. S. *Inorg. Chem.* **1983**, *22*, 1017–1021.

(57) Aguilar, J.; Basallote, M. G.; Gil, L.; Hernández, J. C.; Mañez, M. A.; García-España, E.; Soriano, C.; Verdejo, B. *J. Chem. Soc., Dalton Trans.* **2004**, 94–103.

(49) Wilkins, R. G. *The Study of Kinetics and Mechanism of Reactions of Transition Metal Complexes*; Allyn and Bacon: Boston, 1974.

(50) Curtis, N. F.; Osvath, S. R. *Inorg. Chem.* **1988**, *27*, 305–310.

(51) Chen, L.-H.; Chung, C.-S. *Inorg. Chem.* **1989**, *28*, 1402–1405.

(52) Clifford, T.; Danby, A. M.; Lightfoot, P.; Richens, D. T.; Hay, R. W. *J. Chem. Soc., Dalton Trans.* **2001**, 240–246.

Indeed, a switching process between square pyramidal and trigonal bipyramidal coordination geometries was emphasized by absorption spectrophotometry and EPR. Kinetic data for the formation of mononuclear  $[\text{Cu}(\text{H}_4\text{L}^1)]^{6+}$  complexes revealed a dissociative Eigen–Wilkins mechanism. The acid-catalyzed dissociation processes showed two rate-limiting steps. The first step leads to a bidentate  $\text{Cu}^{2+}$  complex involving an amine and a pyridine group. An efficient acid-catalyzed reaction completes the decomplexation of the monocopper(II) species. The ligand herein described therefore represents the first member of a family of new polyamino derivatives with interesting metal ion coordination properties and potential catalytic behavior.

**Acknowledgment.** Financial support from CTQ2006-15672-CO5-01 (Spain) and Generalitat Valenciana (GV06/258) is gratefully acknowledged. This work was also supported by the Centre National de la Recherche Scientifique (UMR 7177 CNRS-UdS). J.M.Ll. thanks MCYT of Spain for a Ramón y Cajal Contract. A.S.T. thanks the French Embassy in Spain for a Cotutelle grant.

**Supporting Information Available:** Figure S1, distribution diagram for the  $\text{L}^1\text{-H}^+$  system. Figure S2, calculated electronic spectra of the  $\text{L}^1$  protonated species. Figure S3, ES mass spectrum of the  $\text{L}^1$  copper(II) complexes. Figure S4, calculated electronic spectra of the  $\text{CuL}^1$  protonated species. Figure S5, spectrophotometric titrations of  $\text{Cu}_2\text{L}^1$  as function of  $\text{p}[\text{H}]$ . Figure S6, spectrophotometric titrations of  $\text{Cu}_3\text{L}^1$  as function of  $\text{p}[\text{H}]$ . Figure S7, calculated electronic spectra for the  $\text{Cu}_2\text{L}^1$  protonated species. Figure S8, calculated electronic spectra for the  $\text{Cu}_3\text{L}^1$  protonated species. Figure S9, spectrophotometric titrations of the ligand  $\text{L}^1$  by copper(II). Figure S10, variation of the absorption versus time for the formation of copper(II) complex with  $\text{L}^1$  in excess of  $[\text{Cu}(\text{II})]_{\text{tot}}$  at  $\text{p}[\text{H}]$  2.39. Figure S11, distribution diagram of the copper(II) complexes of  $\text{L}^1$  in excess of  $[\text{Cu}(\text{II})]_{\text{tot}}$  at 5.45. Table S1, variation of the pseudo-first order rate constants for the formation of copper(II) complex with  $\text{L}^1$  versus  $[\text{Cu}(\text{II})]_{\text{tot}}$  at  $\text{p}[\text{H}] = 2.39$ . Table S2, variation of the pseudo-first order rate constants for the formation of copper(II) complex with  $\text{L}^1$  versus  $[\text{Cu}(\text{II})]_{\text{tot}}$  at  $\text{p}[\text{H}] = 5.45$ . Table S3, variation of the pseudo-first order rate constants  $k_{\text{obs}1}$  and  $k_{\text{obs}2}$  for the dissociation of  $\text{CuL}^1$  versus  $[\text{HClO}_4]_{\text{tot}}$ . This material is available free of charge via the Internet at <http://pubs.acs.org>.